

SettleFL: Trustless and Scalable Reward Settlement Protocol for Federated Learning on Permissionless Blockchains

Shuang Liang
Shanghai Jiao Tong University
liangshuangde@sjtu.edu.cn

Yang Hua
Queen's University Belfast
Y.Hua@qub.ac.uk

Linshan Jiang
National University of Singapore
linshan@nus.edu.sg

Peishen Yan
Shanghai Jiao Tong University
peishenyan@sjtu.edu.cn

Tao Song*
Shanghai Jiao Tong University
songt333@sjtu.edu.cn

Bin Yao*
Shanghai Jiao Tong University
yaobin@cs.sjtu.edu.cn

Haibing Guan
Shanghai Jiao Tong University
hbguan@sjtu.edu.cn

ABSTRACT

In open Federated Learning (FL) environments where no central authority exists, ensuring collaboration fairness relies on decentralized reward settlement, yet the prohibitive cost of permissionless blockchains directly clashes with the high-frequency, iterative nature of model training. Existing solutions either compromise decentralization or suffer from scalability bottlenecks due to linear on-chain costs. To address this, we present SettleFL, a trustless and scalable reward settlement protocol designed to minimize total economic friction by offering a family of two interoperable protocols. Leveraging a shared domain-specific circuit architecture, SettleFL offers two interoperable strategies: (1) a *Commit-and-Challenge* variant that minimizes on-chain costs via optimistic execution and dispute-driven arbitration, and (2) a *Commit-with-Proof* variant that guarantees instant finality through per-round validity proofs. This design allows the protocol to flexibly adapt to varying latency and cost constraints while enforcing rational robustness without trusted coordination. We conduct extensive experiments combining real FL workloads and controlled simulations. Results show that SettleFL remains practical when scaling to 800 participants, achieving substantially lower gas cost.

PVLDB Reference Format:

Shuang Liang, Yang Hua, Linshan Jiang, Peishen Yan, Tao Song, Bin Yao, and Haibing Guan. SettleFL: Trustless and Scalable Reward Settlement Protocol for Federated Learning on Permissionless Blockchains. PVLDB, XX(X): XXX-XXX, XXXX. doi:XX.XX/XXX.XX

PVLDB Artifact Availability:

The source code, data, and/or other artifacts have been made available at <https://github.com/wizicer/SettleFL>.

*Corresponding author.

This work is licensed under the Creative Commons BY-NC-ND 4.0 International License. Visit <https://creativecommons.org/licenses/by-nc-nd/4.0/> to view a copy of this license. For any use beyond those covered by this license, obtain permission by emailing info@vldb.org. Copyright is held by the owner/author(s). Publication rights licensed to the VLDB Endowment.
Proceedings of the VLDB Endowment, Vol. XX, No. X ISSN 2150-8097.
doi:XX.XX/XXX.XX

1 INTRODUCTION

Federated Learning (FL) enables collaborative model training across distributed participants, yet maintaining long-term participation requires ensuring *collaboration fairness* [25]. To achieve this, the system is expected to address two distinct challenges: *contribution evaluation* and *reward settlement*. Contribution evaluation refers to the algorithmic process of quantifying the value of participant updates, often utilizing methods such as Shapley value estimation [9, 43]. Advanced approaches in this domain may further incorporate contribution verifiability mechanisms to cryptographically prove the correctness of these evaluation results [46]. However, existing works either treat the execution of rewards as a trivial external assumption [43] or restrict rewards to coarse-grained model utility [33]. In open FL environments where no central authority exists, this assumption collapses. Without a credible enforcement mechanism, even the most accurate and verifiable evaluation algorithms become meaningless promises. Consequently, this work explicitly excludes contribution evaluation from its scope, treating it as an upstream input, and focuses exclusively on the unsolved challenge of *reward settlement*, aiming to ensure that decided rewards are settled strictly and immutably without a trusted coordinator.

Enforcing such settlement without trusted intermediaries necessitates blockchain technology [37]. However, the *blockchain trilemma* [38] dictates that maximizing decentralization and security inherently compromises scalability. Since open FL strictly requires a trustless environment, permissionless blockchains emerge as the theoretically optimal infrastructure to maximize censorship resistance and universal verifiability. However, this architectural choice creates a fundamental conflict: the prohibitive cost of on-chain execution directly clashes with the high-frequency, iterative nature of FL [31].

Existing solutions fail to resolve this tension. Approaches utilizing permissioned or hybrid architectures [12, 15] reduce costs but reintroduce trust assumptions via closed consortia or cross-chain bridges, undermining the censorship resistance required for open collaboration. Conversely, state channels [26] suffer from fragmented dispute resolution: their isolated 1-to-1 topology prevents collective security, forcing every participant to individually initiate challenges to secure their funds. Ultimately, these methods compel

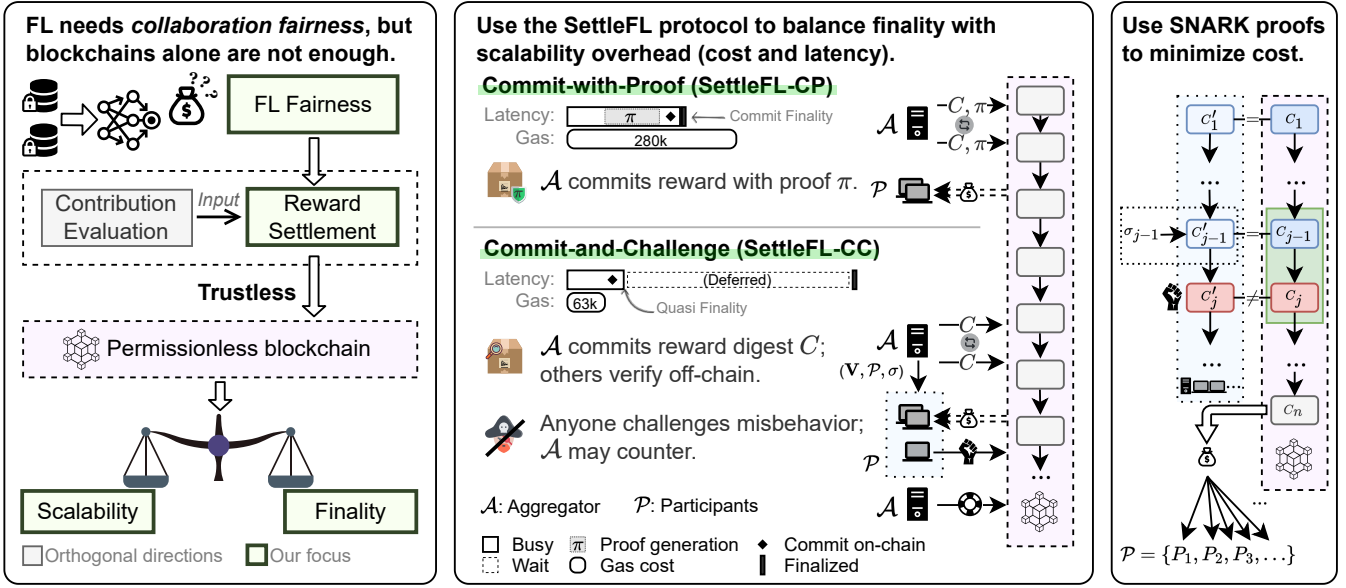


Figure 1: Overview of SettleFL protocol family. Our protocol resolves the conflict between costly on-chain execution and high-frequency FL updates. It navigates the scalability-finality trade-off through two variants: *Commit-and-Challenge* for minimal cost, and *Commit-with-Proof* for instant finality. A shared SNARK architecture flexibly enforces correctness by either guaranteeing validity upfront or resolving disputes with minimal on-chain overhead.

participants to *actively* submit transactions for settlement, causing gas costs to scale linearly with the user base. The core research problem is therefore: *How to design a protocol that enforces reward settlement on permissionless blockchains while minimizing on-chain costs at scale?*

To address this, we present SettleFL, a trustless and scalable reward settlement protocol as illustrated in Figure 1. Designed to bridge the gap between algorithmic fairness and system practicality, SettleFL creates a flexible design space by introducing two interoperable variants within a single protocol family. The *Commit-and-Challenge* variant minimizes costs by adopting an optimistic execution model where the aggregator commits only a cryptographic digest of the reward allocation on-chain. This design allows honest participants to remain passive; they verify data off-chain and are never required to submit transactions unless they detect malpractice. Conversely, for environments requiring immediate guarantees, the *Commit-with-Proof* variant attaches a validity proof, specifically a Succinct Non-interactive ARGument of Knowledge (SNARK) proof, to every commitment, offering instant finality.

While drawing architectural inspiration from blockchain scaling primitives [39], SettleFL fundamentally differs by trading generality for domain-specific efficiency. Unlike general-purpose optimistic rollups that often rely on complex, multi-round interactive dispute games, SettleFL leverages the structured nature of FL rewards to enable a single-shot non-interactive challenge, drastically reducing dispute complexity. Similarly, unlike standard validity rollups that batch heterogeneous transactions arbitrarily, SettleFL aligns verification strictly with FL training rounds. This design enables fine-grained per-round settlement without waiting for external

block-level aggregation, ensuring that the incentive mechanism matches the iterative rhythm of FL.

Our main contributions are as follows:

- We propose a protocol family, SettleFL, that addresses the scalability-finality trade-off in blockchain-based FL. It provides two interoperable variants, namely an optimistic Commit-and-Challenge variant for minimal cost and a Commit-with-Proof variant for instant finality, allowing applications to select the appropriate security model.
- We design a highly optimized SNARK circuit architecture that serves as the foundation for our modular verification mechanism. By employing shared cryptographic gadgets and a specifically designed commitment scheme, this infrastructure efficiently supports both immediate validity proofs and optimistic challenges, enabling the protocol to scale to large participant sets with constant on-chain complexity.
- We demonstrate the system’s practicality through extensive experiments and a live deployment on the Ethereum Sepolia testnet. Results show that SettleFL successfully scales to 800 participants, a scale previously considered impractical for on-chain execution. Notably, it settles rewards for 50 training rounds at a total cost of approximately \$4 (USD), effectively removing the economic barrier for decentralized FL incentives.

2 PRELIMINARY

2.1 Blockchain-based Federated Learning

Blockchain-based Federated Learning (BCFL) integrates blockchain infrastructure into FL workflows to ensure transparency, fairness,

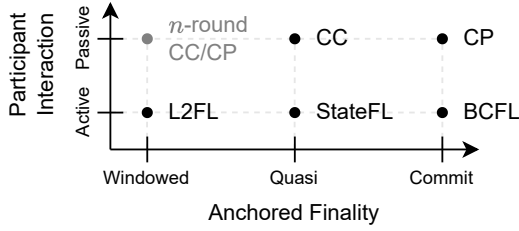


Figure 2: Landscape of Settlement Strategies. Unlike the active baselines L2FL [1], StateFL [26], and BCFL [47] which require user participation, SettleFL enables passive interaction via its two variants, SettleFL-CC (CC) and SettleFL-CP (CP). Notably, if anchored finality is compromised to the windowed stage, the protocol essentially degrades to an n -round batched CC or CP.

and traceability in decentralized training environments. While BCFL encompasses various mechanisms to enhance collaboration fairness, such as contribution evaluation or verifiable computation, our work specifically focuses on *reward settlement*, utilizing the blockchain as an immutable *incentive layer*. In this context, smart contracts *enforce* and *automate* the allocation process, ensuring that rewards are distributed transparently according to predefined rules. However, compared to centralized approaches, a secure permissionless blockchain implementation, referred to as *Layer-1 (L1)*, inevitably introduces significant performance degradation due to the consensus overhead [22].

Anchored Finality. To mitigate L1 performance bottlenecks, existing BCFL frameworks attempt to bypass these limitations through two main approaches. The first relies on *alternative chains* with reduced overhead, including permissioned blockchains [44, 47], sidechains [8, 26], and lightweight independent chains [1, 13]. While efficient, these architectures typically compromise security by depending on weaker consensus models. The second approach utilizes *Layer-2 (L2)* [16] solutions, which we denote as L2FL [1]. L2FL maintains L1 security by enforcing *anchored finality*, where a reward settlement is considered final only after its corresponding state commitment is successfully recorded on the main L1 ledger. Critically, waiting for this cross-layer synchronization to complete imposes an unavoidable time delay, preventing instant reward confirmation.

Interaction. Regardless of the chosen architecture, the efficiency of the system is constrained by the frequency of on-chain operations, defined here as *interaction*. Distinct from standard communication protocols, every on-chain interaction inherently incurs a direct financial cost (i.e., gas) and requires waiting for settlement latency. This overhead scales poorly in FL settings, which typically involve a single aggregator but a vast number of participants. Therefore, as positioned in Figure 2, a critical objective in BCFL design is to minimize *participant interaction* [26, 42]. By enforcing a passive model, SettleFL eliminates user-side gas costs and maximizes scalability, accepting a bounded risk of at most one lost reward.

Rollup Mechanisms. Among L2 architectures, *rollups* represent a dominant subclass distinguished by their requirement to publish transaction data or state commitments directly to the L1, ensuring

data availability. Mainstream rollups employ two distinct verification paradigms. Optimistic rollups operate on a presumption of validity, posting state commitments to L1 subject to a fraud-proof challenge window. This design minimizes immediate computation but necessitates a prolonged dispute period, often lasting days, to ensure security. Conversely, validity rollups enforce correctness via succinct cryptographic proofs (e.g., SNARKs) that are verified by an L1 smart contract. While this approach enables faster settlement compared to optimistic designs, it introduces substantial computational overhead for proof generation.

2.2 SNARKs

SNARKs are cryptographic proof systems that allow a prover to convince a verifier of the validity of a statement in a non-interactive and succinct way. It is defined by the tuple $\text{SNARK} = (\text{Setup}, \text{Prove}, \text{Verify})$. The $\text{Setup}(1^\lambda, C)$ algorithm outputs public parameters pp for circuit C . The $\text{Prove}(pp, x, w) \rightarrow \pi$ algorithm enables the prover to generate a succinct proof π that $C(x, w) = 1$. The $\text{Verify}(pp, x, \pi) \rightarrow \{\text{accept}, \text{reject}\}$ algorithm allows the verifier to check the validity of π on input x . A SNARK satisfies *completeness* (valid proofs are always accepted) and *soundness* (false statements cannot be proven). In what follows, we instantiate our proofs using Groth16 [20], a SNARK that is well supported on blockchains such as Ethereum.

Arithmetic circuits. In SNARKs, a statement is represented as an arithmetic circuit expressed by algebraic constraints, and the prover must show that the witness satisfies all constraints with respect to the public input. The efficiency of proof generation depends on the number of constraints, which can be greatly reduced when the underlying operations are SNARK-friendly, i.e., encodable with few algebraic constraints.

3 SYSTEM OVERVIEW

3.1 System Model

We consider an FL setting involving an aggregator \mathcal{A} and a set of participants $\mathcal{P} = \{P_1, \dots, P_N\}$, who collaboratively train a global machine learning model. In each round r , the aggregator distributes the current global model to all participants, each of whom trains it locally on private data and returns an update to \mathcal{A} . The aggregator then aggregates these updates to produce a new global model and evaluates the contribution of each participant. Based on this evaluation, a reward allocation vector $\mathbf{v}^r = (v_1^r, \dots, v_N^r)$ is derived, where v_i^r denotes the reward associated with participant P_i in round r .

To ensure accountability and enable verifiable reward settlement, the system incorporates a permissionless blockchain \mathbb{B} that serves as a public ledger for recording reward commitments and related state transitions. The aggregator interacts with \mathbb{B} to publish these commitments, while participants can reference on-chain records to verify or challenge the reported results.

3.2 Threat Model

We consider an adversary \mathcal{A}^* who controls the aggregator and may arbitrarily deviate from the protocol to manipulate reward settlement. \mathcal{A}^* can observe all messages and submit inconsistent or fraudulent commitments, but is assumed unable to break cryptographic

primitives or compromise the integrity of the blockchain. Participants may also behave maliciously, for example, by submitting incorrect updates or issuing dishonest challenges. The blockchain \mathbb{B} is assumed to provide consensus security and eventual consistency, ensuring that once a commitment is on-chain, it cannot be reverted or altered. Participants are assumed rational and choose actions that maximize their own reward given the protocol’s payoffs; they tolerate at most one missing reward and, upon detecting aggregator misbehavior, exit the training, securing rewards already recorded on chain and avoiding further loss.

We focus on four representative threats. (1) **Commitment reversal**: \mathcal{A}^* may locally announce a correct commitment and then publish a fraudulent one excluding certain contributions. (2) **Refusal to commit**: \mathcal{A}^* withholds the final commitment on-chain, blocking participants from receiving rewards. (3) **Reward withholding**: \mathcal{A}^* commits the reward but deliberately withholds the final transaction that distributes funds. (4) **Stale challenges**: malicious \mathcal{P}^* may challenge a stale commitment in order to disrupt the system or extract undeserved rewards.¹

3.3 Problem Formulation

We aim to design a protocol Π that ensures trustless and scalable reward settlement under the threat model described in Section 3.2. We formulate this as a stronger setting of *Practical Scalable BCFL*, requiring the protocol to support $N \geq 200$ participants, operate within realistic gas limits, ensure robustness without trusted coordination, and enable participants to passively receive rewards.

To rigorously define the goal, we first establish the definition of BCFL reward enforceability.

DEFINITION 1 (BCFL). Consider an aggregator \mathcal{A} , participants \mathcal{P} , and a blockchain \mathbb{B} . A protocol Π is a BCFL protocol if, for every round r , it specifies a reward vector \mathbf{v}^r and enforces that the payouts are deterministically settled on \mathbb{B} . We define such settlement as having anchored finality when the allocations implied by \mathbf{v}^r become uniquely determined and are guaranteed to be distributed on \mathbb{B} for all eligible participants.

To maximize system availability and alleviate the operational burden on participants, we enforce a strict constraint of *passive interaction*, defined as allowing participants to receive rewards without initiating direct interactions with the blockchain. Under this constraint, we formalize the efficiency objective as a minimization of the *Total Economic Friction*.

DEFINITION 2 (TOTAL ECONOMIC FRICTION). Let Π denote a BCFL protocol that supports passive interaction. The optimization objective is to minimize the weighted sum of explicit financial costs, protocol-enforced delays, and computational latencies:

$$\min_{\Pi \in \text{BCFL}} \mathcal{F}(\Pi) = w_g \cdot C_g(\Pi) + w_p \cdot T_p(\Pi) + w_c \cdot T_c(\Pi), \quad (1)$$

where:

- $C_g(\Pi)$ represents the on-chain execution cost.

- $T_p(\Pi)$ denotes the mandatory waiting period enforced by the protocol, such as a dispute window.
- $T_c(\Pi)$ denotes the physical runtime required to generate validity proofs.
- w_g, w_p, w_c are task-specific sensitivity weights.

Note that throughout this paper, *settlement* refers to the cryptographic finalization of state \mathbf{v}^r , while *distribution* denotes the subsequent execution of asset transfers. SettleFL focuses on optimizing settlement as the essential prerequisite for distribution.

3.4 Solution Overview

To minimize \mathcal{F} defined in Equation 1, we analyze the behavior of the cost function at the boundaries of the design space. Since hybrid approaches incur verification costs without removing the need for a dispute window, they fail to minimize either the financial or temporal friction. Therefore, the design space collapses into two distinct variants, each zeroing out a specific latency component.

Boundary Strategies. We define the two boundary strategies, Π_{opt} and Π_{val} , based on which latency term they eliminate:

- **Optimistic Strategy (Π_{opt}):** This strategy prioritizes execution efficiency by eliminating computational latency ($T_c \rightarrow 0$). However, to maintain security without verification, it must enforce a substantial protocol delay, denoted as Δ_w . With small overhead gas denoted as C_b , the total friction is thus dominated by the waiting cost:

$$\mathcal{F}(\Pi_{\text{opt}}) \approx w_g \cdot C_b + w_p \cdot \Delta_w.$$

- **Validity Strategy (Π_{val}):** This strategy prioritizes immediate finality by eliminating protocol delay ($T_p \rightarrow 0$). To achieve this, it incurs the physical time for proof generation, denoted as Δ_p , and the higher gas cost C_v for verification. The total friction is thus dominated by the verification overhead:

$$\mathcal{F}(\Pi_{\text{val}}) \approx w_g \cdot C_v + w_c \cdot \Delta_p.$$

A rational system design should adopt the Validity Strategy if and only if it yields a lower total friction than the Optimistic Strategy, i.e., $\mathcal{F}(\Pi_{\text{val}}) < \mathcal{F}(\Pi_{\text{opt}})$. Substituting the expressions above:

$$w_g \cdot C_v + w_c \cdot \Delta_p < w_g \cdot C_b + w_p \cdot \Delta_w.$$

Rearranging the terms to group the cost components yields the *Fundamental SettleFL Inequality*:

$$\underbrace{w_p \cdot \Delta_w}_{\text{Opportunity Cost}} > \underbrace{w_g \cdot (C_v - C_b) + w_c \cdot \Delta_p}_{\text{Verification Overhead}}. \quad (2)$$

This inequality provides the rigorous logic for variant selection: the system should switch to validity strategy only when the implicit *opportunity cost* of waiting exceeds the explicit *verification overhead*.

The Proposed Solutions. Guided by this derivation, we propose SettleFL, which comprises two interoperable protocols and explicitly implements these two boundary strategies to cover the full range of FL scenarios: (1) SettleFL-CC, which implements Π_{opt} : Designed for the regime where the inequality fails (e.g., cost-sensitive tasks). This protocol utilizes a *Commit-and-Challenge* mechanism to minimize on-chain costs, accepting a challenge window to secure

¹Our model focuses on reward enforceability in blockchain-based FL. We do not consider orthogonal concerns such as participant-level privacy leakage, model misuse or theft, delegated model training with misreported contributions [21], or aggregator-participant collusion [24].

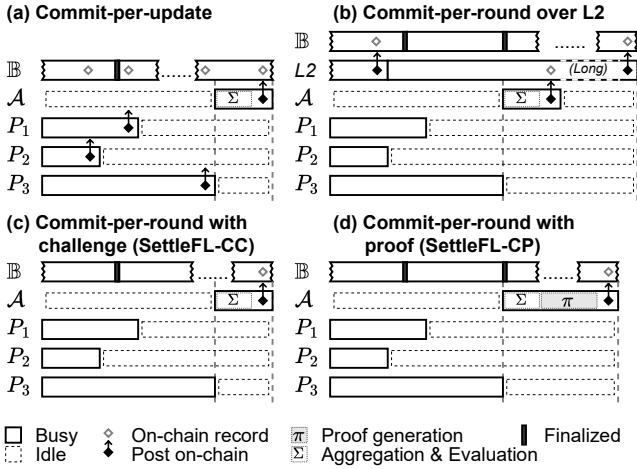


Figure 3: Timeline Analysis of Latency. By synchronizing settlement with the aggregation cycle, SettleFL eliminates extrinsic delays, bounding latency to the theoretical minimum.

the system. (2) SettleFL-CP, which implements Π_{val} : Designed for the regime where the inequality holds (e.g., time-sensitive tasks). This protocol utilizes a *Commit-with-Proof* mechanism to provide immediate settlement, justifying the computational and gas premium for instant liquidity.

Both protocols are built upon a shared set of off-chain circuit gadgets and on-chain functions, ensuring that SettleFL remains modular.

Settlement Timeline. To intuitively illustrate how SettleFL minimizes \mathcal{F} compared to prior paradigms, Figure 3 presents a timeline analysis of settlement latency. Traditional approaches typically suffer from either high interaction overhead due to frequent commit-per-update mechanisms (Figure 3a), or extrinsic settlement delays imposed by generic L2 block times (Figure 3b). In contrast, both variants of SettleFL synchronize settlement strictly with the FL aggregation cycle. Whether issuing a single per-round commitment instantly (Figure 3c) or waiting solely for proof generation (Figure 3d), the design eliminates all other extrinsic protocol delays, bounding the total latency to the theoretical minimum.

4 PROTOCOL DESIGN

We propose a protocol family whose key distinction lies in the finality mechanism. This design constitutes the primary contribution of this paper.

4.1 Architecture

To implement the proposed protocol family, we design a hierarchical architecture, illustrated in Figure 4. The architecture is built upon a common base used by both protocols. At the lowest level, a unified *commitment scheme* (Section 4.2) serves as the foundation for state representation. Building on this, we define a set of cryptographic *circuit gadgets* (Section 4.4) that act as the construction primitives for all circuits. These primitives are assembled into the

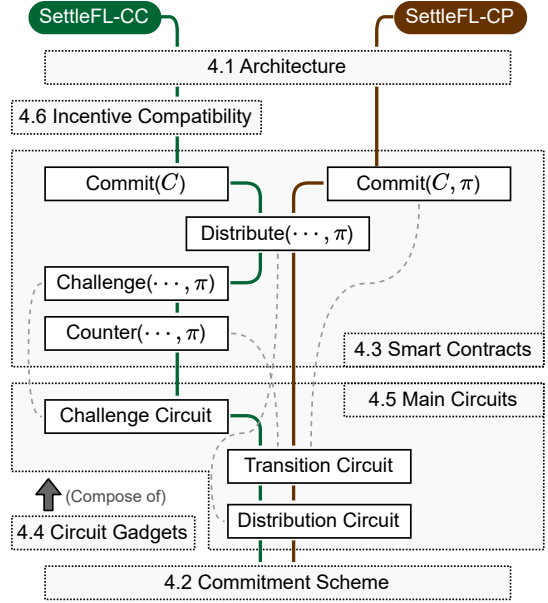


Figure 4: System architecture overview. Shared cryptographic primitives underpin the architecture, enabling specialized modules to enforce distinct security assumptions.

core *transition* and *distribution circuits* (Section 4.5), while the smart contract (Section 4.3) shares the fundamental *distribute* logic.

Leveraging this shared hierarchy, the architecture branches with specialized modules to enforce specific security assumptions. SettleFL-CP utilizes a verifiable *commit* function that strictly verifies the validity of the reward settlement transition. In contrast, SettleFL-CC employs an optimistic contract designed for the *Commit-and-Challenge* workflow. This branch extends the shared circuits with a specialized *challenge circuit*, reuses the transition circuit as a *counter circuit*, and incorporates an additional *incentive compatibility* layer (Section 4.6) to secure the dispute window against malicious actors.

Adaptation from Rollup Mechanisms. While SettleFL draws architectural inspiration from the generic Optimistic and Validity Rollups introduced in Section 2.1, a direct application of standard rollup stacks would restrict the system to *windowed finality*. As positioned in the settlement landscape in Figure 2, naively increasing the commitment frequency to a per-round basis to achieve *quasi* or *commit* finality is impractical, as standard rollups are optimized for general-purpose workloads, incurring prohibitive gas costs and verification latency at high frequencies [1].

To overcome this, SettleFL trades general-purpose execution for domain-specific efficiency tailored to FL workloads. For the validity workflow, our specialized commitment scheme significantly accelerates proof generation by streamlining circuit logic. For the optimistic workflow, it enables dispute resolution within a single interaction round, bypassing the complex multi-round interactive fraud proofs typical in traditional optimistic rollups.

Workflow The SettleFL-CP and SettleFL-CC protocols share a unified workflow sequence across multiple FL rounds, as illustrated in

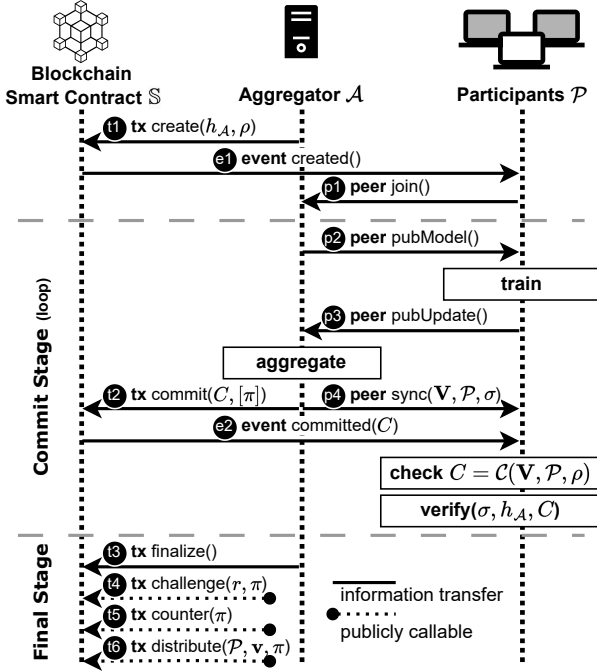


Figure 5: System Workflow. **tx**: on-chain transaction; **event**: smart contract event; **peer**: off-chain peer communication.

Figure 5. The \mathcal{A} t1 creates a task by staking rewards and publishing metadata on-chain. Upon the e1 event, one of \mathcal{P} , denoted as P_i , p1 joins a task of interest via the peer-to-peer network. Each round begins when the \mathcal{A} p2 broadcasts the global model. P_i trains locally and p3 publishes an update to the \mathcal{A} . After collecting updates, the \mathcal{A} aggregates them and t2 commits a compressed state to the blockchain. For SettleFL-CP, this commitment acts as a validity proof, whereas SettleFL-CC requires only the state data. The \mathcal{A} also p4 synchronizes the latest state and signature with P_i . Upon the e2 commitment event, P_i validates its update via C and signature verification, then decides whether to continue or drop out. After the final round, the \mathcal{A} t3 marks the task as complete. In the SettleFL-CC workflow, if any inconsistency is found, P_i or any other user may t4 challenge the commitment with a SNARK proof. The \mathcal{A} must then t5 respond with a counter-proof before the dispute window closes. Finally, the \mathcal{A} or any user may t6 trigger reward distribution. This action is available immediately for SettleFL-CP, while SettleFL-CC requires the dispute window to expire without valid challenges.

4.2 Commitment Scheme

The foundation of our protocol family centers on the unified notion of a *commitment*: one can prove knowledge of its content or the correctness of its transition, which together underpin reward enforcement in both validity and optimistic workflows.

Rationale. Blockchain offers a natural foundation for trustless reward settlement in FL. However, on-chain execution remains costly due to gas cost and contract size limits (e.g., 24KB on Ethereum),

creating scalability challenges for large participant sets. While alternative chain solutions reduce these costs, they often trade off trust assumptions.

We instead explore protocol-level strategies that minimize interaction while preserving decentralization. As illustrated in Figure 6, binding commitments to participants can be realized through several approaches, ranging from unilateral commits with no authentication, to fully aggregated multi-signatures. While stronger cryptographic binding (e.g., multi-signature) can achieve immediate finality, it often incurs high latency and coordination overhead, limiting scalability.

Our protocol therefore adopts the **aggregator-signed broadcast model**, where the aggregator signs each round’s commitment and participants verify it off-chain. This choice avoids costly multi-party coordination while still providing strong attribution, but accepts a bounded risk: if the aggregator misbehaves, at most one round of rewards may be lost before participants can exit. This trade-off enables light on-chain logic, low latency in optimistic execution, and scalable support for large FL jobs.

Cryptographic Primitives. In the circuit, we use Poseidon [19], a SNARK-friendly hash function, with notation $H_k(\cdot)$ for Poseidon of arity k . For signatures, we adopt EdDSA [6]; since an EdDSA public key consists of two curve coordinates, we use its hash $h_{\mathcal{A}} = H(A_x, A_y)$ as the aggregator’s on-chain identifier to minimize public signals and gas cost. In the Solidity-based SettleFL-CC-Sol implementation, Keccak and ECDSA are used instead, and we write $H(\cdot)$ and $\text{sign}(\cdot)$ for generic hash and signature.

Notation. We use $[T]$ to denote the set $\{0, 1, \dots, T-1\}$. $1[\cdot]$ is the indicator function, which equals 1 if the condition is true and 0 otherwise. We define four constants: T is the number of rounds, N is the number of participants, B is the batch size, and κ is the arity of the Poseidon hash function.

Commitment. An aggregator \mathcal{A} is required to publish on-chain its public key hash $h_{\mathcal{A}}$, which uniquely binds its identity. A set of participants $\mathcal{P} = \{P_1, \dots, P_N\}$ collaboratively train a global model, where each P_i is identified by its address. In each round r , \mathcal{A} commits a reward allocation vector $\mathbf{v}^r = (v_1^r, \dots, v_N^r)$, where v_i^r is the reward assigned to P_i .

A commitment C is defined as

$$C = H(H(\mathbf{V}), H(\mathcal{P}), \rho),$$

where $\mathbf{V} = \{\mathbf{v}^0, \dots, \mathbf{v}^{T-1}\}$ is the reward allocation matrix, H is the hash function, and ρ is a random salt. If the effective number of rounds or participants is less than the predefined maximum T and N , \mathbf{V} is padded with 0 since the circuit size is fixed at compile time. \mathcal{A} signs C with its private key, producing $\sigma_C = \text{sign}_{\mathcal{A}}(C)$. Each round, C is posted on-chain, while σ_C is broadcast to participants. Participants verify σ_C against \mathcal{A} to ensure authenticity.

If anyone detects inconsistency, they can issue a challenge by providing a SNARK proof that references the last valid commitment at round $r-1$. To protect \mathcal{A} from spurious challenges, it may counter by presenting a SNARK proof of a valid transition from C^{r-1} to C^r .

Implementation. Because the protocol family shares the core verification logic, implementing these shared components natively

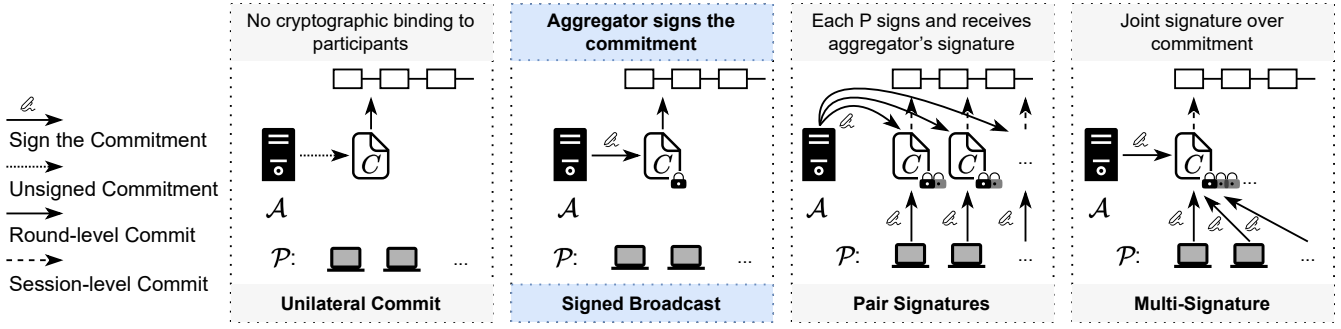


Figure 6: Design space of cryptographic binding mechanisms for reward enforcement. We show four approaches with increasing stronger binding. We adopt the second, using *aggregator-signed commitments* to balance cost, scalability, and verifiability.

instantiates both workflows. The logic is written directly in Solidity for SettleFL-CC-Sol, and as Groth16 SNARK circuits for both SettleFL-CC and SettleFL-CP. In Solidity, no padding is required since inputs are handled natively by the EVM.

4.3 Smart Contract

The smart contract serves as the core of reward enforcement in SettleFL, implemented through a state-driven design that we describe in terms of its state machine and contract logic.

State Machine. As shown in Figure 7, the contract implements a state machine coordinating the job lifecycle: commitment, reward initialization, optional challenge/counter, and final settlement through one-shot (1s) or multi-shot (ms) distribution. Most transitions are externally triggered, except for timeout-based transitions (e.g., delayed entry into the distribution phase).

Since only the commitment is on-chain, proofs are required for committing, challenging, or distributing. In both SettleFL-CP and SettleFL-CC, a SNARK proof is generated by a SNARK prover; in SettleFL-CC-Sol, the proof consists of all original data used to compute the commitment.

Smart Contract Logic. Algorithm 1 defines the logic of \mathbb{S} . It maintains the \mathcal{A} 's public key hash $h_{\mathcal{A}}$, current round r , salt ρ , unlock time t_{unlock} , distribution count ξ , verifier function $\text{verify}_{(\cdot)}$, commitment history $C = [C^1, \dots, C^{r-1}]$, distribution mode $\mu \in \{\text{one-shot}, \text{multi-shot}\}$, current status $\tau \in \{\tau_{\text{Committed}}, \tau_{\text{RewardInit}}, \tau_{\text{Challenged}}, \tau_{\text{Distributing}}\}$, the last successfully challenged round r_{last} , and the protocol variant $\gamma \in \{\gamma_{\text{Challenge}}, \gamma_{\text{Proof}}\}$. In γ_{Proof} , `commit` requires a succinct proof π_{commit} to be verified. `challenge` and `counter` are enabled in $\gamma_{\text{Challenge}}$. Functions with *onlyOwner* are owner restricted.

4.4 Circuit Gadgets

We present a set of reusable gadgets that serve as building blocks for the verifier circuit. Throughout, we denote constraints by $\langle \cdot \rangle$, indicating that the enclosed relation must hold in the proof system's field. Within a constraint, "=" expresses equality to be enforced, while " \leftarrow " denotes assignment of a value, with the resulting equality enforced implicitly.

The detailed constraint specifications are provided in Appendix A; here we focus on the design rationale and semantics.

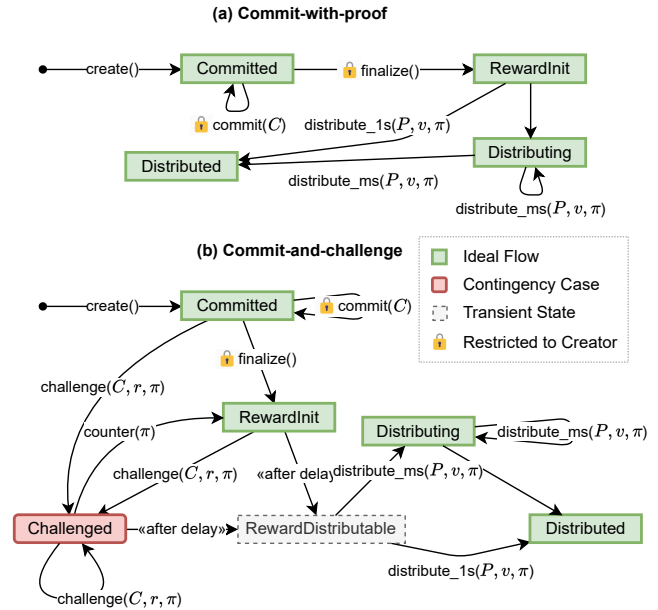


Figure 7: Contract state transitions. In (b) Commit-and-challenge, if a dispute exists, challenges are allowed at any point before distribution. The protocol follows either a multi-shot (ms) or one-shot (1s) path based on the chosen distribution method.

Rationale. We opt for a domain-specific architecture over a generic Zero-Knowledge Virtual Machine (zkVM) [5] to avoid prohibitive computational overhead. First, supporting generic instructions makes zkVM circuits orders of magnitude larger than our tailored design. Second, SettleFL uses SNARK-friendly primitives like Poseidon and EdDSA. A Poseidon hash requires only about 300 constraints, compared to 150,000 for Keccak-256 [2]. Third, by exploiting the fixed structure of FL reward matrices, our LPI and BATCHEXTRACTOR gadgets achieve $O(T)$ round selection and $O(N)$ participant extraction with linear constraint counts. These optimizations reduce proof generation time from minutes to seconds, making per-round commitments economically viable.

Algorithm 1: Smart Contract \mathbb{S} for Π_{ccFL}

```
1 function constructor( $h_{\mathcal{A}}, \rho, \mu, \gamma$ ) public
2    $C \leftarrow []$ ,  $r \leftarrow 1$ ,  $r_{\text{last}} \leftarrow 2$ ,  $\tau \leftarrow \tau_{\text{Committed}}$ ;
3 function commit( $C, [\pi_{\text{commit}}]$ ) public onlyOwner
4   assert  $\tau \in \{\tau_{\text{Committed}}\}$ ;
5   if  $\gamma = \gamma_{\text{Proof}}$  then
6     assert  $\text{verify}_{\text{transition}}(r, C^{r-1}, C, h_{\mathcal{A}}; \pi_{\text{commit}})$ ;
7   append  $C$  to  $C$ ;
8    $r \leftarrow r + 1$ ;
9 function finalize() public onlyOwner
10  assert  $\tau \in \{\tau_{\text{Committed}}, \tau_{\text{Challenged}}\}$ ;
11   $\tau \leftarrow \tau_{\text{RewardInit}}$ ,  $t_{\text{unlock}} \leftarrow \text{block.timestamp} + \Delta$ ;
12 function challenge( $r', \pi_{\text{challenge}}$ ) public
13  assert  $\gamma = \gamma_{\text{Challenge}}$ ;
14  assert  $\tau \in \{\tau_{\text{Committed}}, \tau_{\text{RewardInit}}, \tau_{\text{Challenged}}\}$ ;
15  assert  $r' > r_{\text{last}}$ ;
16  assert  $\text{verify}_{\text{challenge}}(r', C^{r'-2}, h_{\mathcal{A}}; \pi_{\text{challenge}})$ ;
17   $r_{\text{last}} \leftarrow r'$ ;  $\triangleright$  rounds  $< r'$  are stale
18   $\tau \leftarrow \tau_{\text{Challenged}}$ ,  $t_{\text{unlock}} \leftarrow \text{block.timestamp} + \Delta$ ;
19 function counter( $r', \pi_{\text{counter}}$ ) public
20  assert  $\gamma = \gamma_{\text{Challenge}}$ ;
21  assert  $\tau \in \{\tau_{\text{Challenged}}\}$ ;
22  assert  $r' \geq 3$ ;
23  assert  $\text{verify}_{\text{transition}}(r' - 1, C^{r'-2}, C^{r'-1}, h_{\mathcal{A}}; \pi_{\text{counter}})$ ;
24   $\tau \leftarrow \tau_{\text{RewardInit}}$ ,  $t_{\text{unlock}} \leftarrow \text{block.timestamp} + \Delta$ ;
25 function distribute( $\vec{p}, \vec{s}, \pi_{\text{distribute}}$ ) public
26  assert  $\tau \in \{\tau_{\text{RewardInit}}, \tau_{\text{Challenged}}\}$ ;
27  assert  $\text{block.timestamp} \geq t_{\text{unlock}}$ ;
28  assert  $\text{verify}_{\text{distribute}}(r - 1, C^{r-1}, h_{\mathcal{A}}, \vec{s}, \vec{p}; \pi_{\text{distribute}})$ ;
29  for  $i = 1$  to  $|\vec{p}|$  do
30     $\text{transfer}(p_i, s_i)$ ;
31  if  $\mu = \text{multi-shot}$  then
32     $\xi \leftarrow \xi + B$ ;
33     $\tau \leftarrow \tau_{\text{Distributed}}$  if  $\xi \geq |\mathcal{P}|$  else  $\tau_{\text{Distributing}}$ ;
34  else
35     $\tau \leftarrow \tau_{\text{Distributed}}$ ;  $\triangleright$  In one-shot,  $\vec{p} = \mathcal{P}$ 
```

Length-Padded Indicator (LPI). $\text{LPI}(x)$ takes an integer x and produces a binary vector of length T with the first x entries set to 1 and the rest set to 0. Thus $\text{LPI}(x) = (\{1\}^x, \{0\}^{T-x})$. This vector is mainly used as a prefix selector for rounds or batches. The constraints enforce three properties: the sum of outputs equals x , each entry is boolean, and there is exactly one $1 \rightarrow 0$ transition. These constraints ensure a scalable $O(T)$ construction.

Zero Comparator (IsZERO). The $\text{IsZERO}(x)$ gadget outputs $y \in \{0, 1\}$ indicating whether $x = 0$. It uses an auxiliary witness inv , which equals 0 if $x = 0$ and x^{-1} otherwise. This trick allows checking equality to zero with only two constraints.

Modular Hash (H_M). Poseidon supports only a bounded arity up to a maximum of 16 due to best security practices; therefore, we set $\kappa = 16$ as the default. We therefore chunk a long vector (x_1, \dots, x_N) into groups of at most $\kappa - 1$ elements, and iteratively absorb them into

a chained hash state seeded with ρ . This *modular hash* ensures that any input length can be processed, while minimizing the number of Poseidon hashes reduces per-element cost.

Batch Extractor (BATCHEXTRACTOR). Given a sequence \vec{x} of length N , a batch size B , and an index a , $\text{BATCHEXTRACTOR}(\vec{x}, a) = (x_{aB}, \dots, x_{aB+B-1})$ outputs the a -th batch of size B . To reduce constraints, we introduce an intermediate selection matrix enabled by IsZERO , leading to linear complexity in N instead of exponential naive conditional selection.

Vectorization (vec). For hashing purposes, a reward matrix $V \in \mathbb{F}^{N \times T}$ is serialized into a one-dimensional vector in row-major order: $\text{vec}(V) = (V_{0,0}, V_{0,1}, \dots, V_{0,T-1}, V_{1,0}, \dots, V_{N-1,T-1})$. This ensures a canonical ordering before applying the modular hash.

Matrix Sum Row (SUMROW). Given a LPI vector \vec{r} , this gadget extracts the contributions of each participant across all rounds from a reward matrix V to a vector \vec{y} .

Matrix Round Mask Check (MASKCHECK). This gadget ensures V is nonzero only in the selected round. We enforce $\langle V_{i,t} \cdot (1 - r_t) = 0 \rangle, \forall (i, t) \in [N] \times [T]$, to ensure consistency with the LPI vector \vec{r} .

Public Key Digest (H_{PK}). To compress public signals to reduce on-chain gas cost, the aggregator's digest is $h_{\mathcal{A}} = H_{PK}(\mathbf{A}) = H_2(\mathbf{A}_x, \mathbf{A}_y)$, reducing two field elements to one hash output.

Verify Commitment (VERIFYCOMMITMENT). A wrapper gadget that combines vectorization, modular hashing, and EdDSA signature verification. It outputs the canonical commitment C and checks that the aggregator's signature σ_C on C is valid under its public key.

4.5 Main Circuits

By composing the above gadgets, we obtain a set of circuits that capture the essential actions of our protocol. Together, they form a closed system: commitments can be published, challenged, countered, and finally distributed, all with succinct verification and bounded circuit complexity. For completeness, the pseudocode of these verifiers is provided in Appendix B, where underlined inputs or outputs are public and all others are private.

Notably, all circuits compute and output a public key aggregation hash $h_{\mathcal{A}}$ derived from \mathbf{A} to bind the operations to a specific participant group, and they utilize a private ρ in the commitment verification to ensure cryptographic hiding properties. We then describe the role of each circuit in the protocol and how they jointly form a closed and verifiable system.

Transition Verifier. This circuit instantiates $\text{verify}_{\text{transition}}$ and checks that two consecutive commitments (C_t, C_{t+1}) are consistent. It ensures that the reward matrix V_2 for round $t + 1$ is valid using a MASKCHECK gadget, and that both commitments are correctly verified using their respective signatures and the shared ρ . Since C_t is derived directly as a slice of the later matrix, and similarly, its participant vector \vec{p}_1 is derived from \vec{p}_2 via LPI filtering, their validity does not need to be rechecked from scratch. This verifier is used in the *commit* action of SettleFL-CP and the *counter* action of SettleFL-CC .

Challenge Verifier. This circuit instantiates $verify_{\text{challenge}}$ and proves knowledge of the data underlying a given commitment C , together with a valid signature and ρ . It additionally utilizes MASKCHECK to ensure the matrix V accurately belongs to the claimed round. It does not by itself prove misbehavior; rather, it ensures that a challenger can faithfully reconstruct the disputed state. Whether the commitment is actually inconsistent is determined only when a *counter* action provides a transition proof.

Distribution Verifier. This circuit instantiates $verify_{\text{distribute}}$ and besides commitment verification, computes the participant-level reward vector for a specific batch b . It sums the reward matrix along the selected round into a vector \vec{s} , and utilizes a BATCHEXTRACTOR to extract the relevant subset of participants \vec{p}_p and their corresponding rewards \vec{s}_p . These public outputs can be directly used to settle payments in the *distribute* action.

4.6 Incentive Compatibility

While SettleFL-CP relies on cryptographic soundness, SettleFL-CC achieves rational security through economic incentives. To guarantee rational security in the dispute resolution process, we first formalize the concept of *incentive compatibility (IC)*.

DEFINITION 3 (INCENTIVE COMPATIBILITY). *A protocol is incentive compatible if for every player $i \in M$, assuming all other players follow the protocol, the honest strategy s_i^* maximizes player i 's utility:*

$$u_i(s_i^*, s_{-i}^*) \geq u_i(s'_i, s_{-i}^*) \quad \forall s'_i \in \mathcal{S}_i,$$

where \mathcal{S}_i is the strategy space of player i , and $u_i(s_i, s_{-i})$ denotes i 's utility under strategy profile (s_i, s_{-i}) .

Game Model. To evaluate IC, we model the interaction as a static complete-information normal-form game [10]:

$$\mathcal{G} = (M, \{\mathcal{S}_i\}_{i \in M}, \{u_i\}_{i \in M}).$$

The player set is $M = \{\mathcal{A}, P_1, \dots, P_N\}$. The aggregator's strategy space $\mathcal{S}_{\mathcal{A}}$ includes honest execution, tampering with rewards, or aborting. A participant's strategy space \mathcal{S}_{P_i} includes honestly verifying and challenging when justified, submitting malicious challenges, or remaining passive.

Under this formulation, we establish that mutual honest behavior constitutes a Nash Equilibrium [36].

THEOREM 1 (NASH EQUILIBRIUM UNDER RATIONALITY). *If all players are rational and protocol parameters are set properly, then the strategy profile $(s_{\mathcal{A}}^{\text{honest}}, s_{P_1}^{\text{honest}}, \dots, s_{P_N}^{\text{honest}})$ forms a Nash equilibrium of \mathcal{G} .*

In a real deployment, a player's utility u_i is determined by a complex set of parameters, including model rewards, task bonuses, slashing penalties, and on-chain execution costs. However, as detailed in our formal game-theoretic analysis in Appendix C, ensuring the equilibrium mathematically reduces to a single fundamental condition: $P_{\mathcal{A}}^{\text{slash}} > C_i^{\text{gas}}$.

Intuitively, the aggregator has no incentive to tamper because dishonest commitments will be challenged and penalized. For a participant, submitting a malicious challenge is irrational as it will be countered and penalized. Therefore, the only rational deviation for a participant is to remain passive to save verification costs. To ensure honest verification strictly dominates passive behavior, the

Table 1: Characteristics of datasets.

Dataset	Samples	Classes	Task
MNIST [11]	70,000	10	image classification
Fashion-MNIST [45]	70,000	10	image classification
CIFAR-10 [29]	60,000	10	image classification
Bank [35]	45,211	2	tabular data classification
Cora [34]	2,708	7	graph node classification
Twitter [17]	1,194,723	2	text classification

potential slashing bounty $P_{\mathcal{A}}^{\text{slash}}$ awarded for catching a malicious aggregator must strictly outweigh the gas cost C_i^{gas} required to submit the challenge on-chain.

5 EXPERIMENTAL EVALUATION

We evaluate SettleFL through experiments coupled with both local and permissionless blockchain deployments. Both SettleFL-CC and SettleFL-CP are implemented as distinct modes within a single smart contract. Furthermore, for brevity in the figures throughout this section, we use the abbreviations CC and CP to denote SettleFL-CC and SettleFL-CP, respectively.

FL experiments primarily use the MNIST dataset [11], which serves as the main benchmark for end-to-end evaluation. Additional experiments are included to assess generality across all datasets listed in Table 1. Each dataset follows its canonical train/test split; Twitter follows LEAF [7]. We use LeNet-5 [30] for MNIST, a lightweight 4-layer CNN [18] for Fashion-MNIST, ResNet-20 [23] for CIFAR-10, a 3-layer MLP [18] for Bank, a 2-layer GCN [28] for Cora, and FastText [27] for Twitter.

Blockchain experiments are conducted on a local Ethereum-compatible testnet (Hardhat), while end-to-end validation is additionally deployed on the public Ethereum testnet (Sepolia). SNARK circuits are written in Circom [4] and verified using Groth16 via snarkjs [3]. The simulation framework is built with Node.js, incorporating TensorFlow.js [40] for local training and ethers.js for contract interaction. All experiments are conducted on a server with dual Intel Xeon CPUs, 512 GB RAM and eight NVIDIA RTX 4090 GPUs, running Ubuntu 22.04.

5.1 End-to-End Protocol Validation

We validate the end-to-end functionality of SettleFL through real blockchain deployments on the public Ethereum Sepolia network, which provides realistic gas costs, latency, and contract behavior. This setup closely approximates real-world conditions while isolating protocol correctness and scalability from infrastructural variability.

All \mathcal{P} join the task, receive the global model, perform local training, and submit updates. Depending on the chosen variant, the \mathcal{A} either commits a reward allocation subject to challenge in SettleFL-CC or commits a validity proof for immediate settlement in SettleFL-CP.

Training Performance. Participants are emulated on a single server for controllability, performing local training and aggregation as in standard FL. The aggregator commits round-level reward allocations on-chain and broadcasts updated global models off-chain.

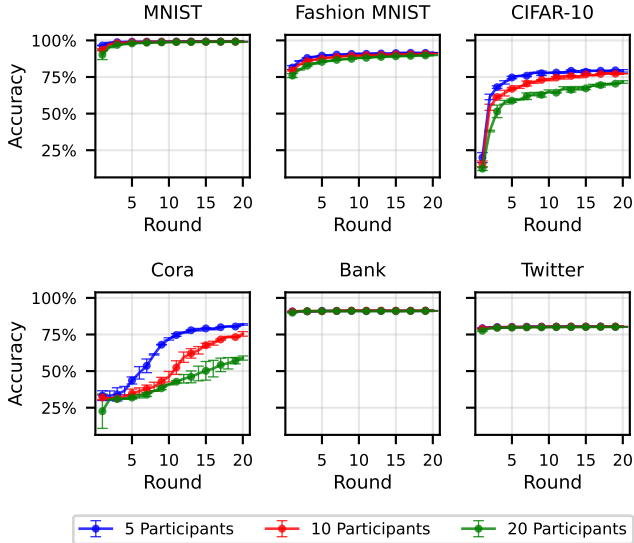


Figure 8: End-to-end protocol accuracy over training rounds under different participant counts. Results use a default learning rate of 0.001, a batch size of 32, and 2 local epochs per round, except for Cora (learning rate 0.015, 10 local epochs) and Twitter (1 local epoch).

We evaluate accuracy progression across 20 training rounds under varying participant counts (5–20). Figure 8 reports results on MNIST, Fashion-MNIST, and CIFAR-10. Both protocol variants share the same off-chain training logic, achieving accuracy comparable to standard FL. This confirms that neither the reward enforcement mechanism of SettleFL-CC nor the proof generation of SettleFL-CP interferes with the model accuracy.

Realistic Deployment. To evaluate the protocol’s scalability and practicality under realistic blockchain conditions, we deployed SettleFL on the Sepolia testnet. Specifically, both SettleFL-CC and SettleFL-CP are evaluated on the MNIST dataset with 800 \mathcal{P} over 50 training rounds. The representative SettleFL-CC deployment ($0\text{xca7b} \dots^2$) achieves a final accuracy of 94.55%. The representative SettleFL-CP deployment ($0\text{x124c} \dots^3$) successfully enforces strict cryptographic verification while maintaining equivalent model convergence.

Table 2 summarizes the gas cost breakdown for both variants. These deployments incur total costs of 0.0028 ETH for SettleFL-CP and 0.0021 ETH for SettleFL-CC, corresponding to approximately \$5.54 and \$4.00, respectively. As theoretically analyzed in previous sections, the fundamental divergence between the two variants lies in the commit operation. For SettleFL-CC, each commit incurs minimal gas overhead, with the trade-off being the potential necessity of challenge and counter operations to resolve disputes. Conversely, SettleFL-CP achieves immediate finality upon submission. It securely validates the update via proof verification, entirely eliminating the need for interactive dispute resolution. These empirical results directly validate our earlier claims regarding the

²<https://sepolia.etherscan.io/address/0xca7b84856557a065C82f6425E374f2912094EDA6>

³<https://sepolia.etherscan.io/address/0x124c8F01728ea88b19B9CFd3B4a5981858A425F8>

Table 2: Cost breakdown comparison of representative Sepolia deployments for SettleFL. (800 \mathcal{P} , 50 rounds on MNIST)

Operation	SettleFL-CP		SettleFL-CC	
	mETH	USD	mETH	USD
create	0.012	0.02	0.012	0.02
commit (per call)	0.021	0.04	0.005	0.01
commit (50× total)	1.066	2.08	0.239	0.47
finalize	0.005	0.01	0.005	0.01
challenge	–	–	0.021	0.04
counter	–	–	0.020	0.04
distribute-ms (per call)	0.110	0.21	0.110	0.21
distribute-ms (16× total)	1.757	3.43	1.757	3.43
Total	2.841	5.54	2.054	4.00

Gas price: 0.075 gwei (ETH 7-day median, Feb 14–20, 2026).

ETH/USD: 1,950 (snapshot on Feb 20, 2026).

Note: Costs are in USD and mETH (1 mETH = 0.001 ETH).

trade-offs. Furthermore, they provide a clear guideline for future deployment: SettleFL-CC is preferable for scenarios prioritizing minimal routine on-chain execution costs, whereas SettleFL-CP is better suited for applications demanding strict cryptographic certainty and non-interactive finality.

5.2 Robustness Against Misbehavior

We evaluate the robustness of SettleFL-CC under adversarial behavior from both aggregators and challengers. In the first scenario, a malicious aggregator commits an incorrect model update. Once challenged, the aggregator fails to produce a valid counter-proof and is thereby disqualified. The challenger incurs a one-time cost of approximately 27.5k gas to initiate the challenge.

In the second scenario, a challenger repeatedly attempts to disrupt the protocol by submitting stale proofs from earlier rounds. The initial challenge consumes about 27.5k gas, while each subsequent attempt costs roughly 25.7k gas. The aggregator, upon issuing a valid counter, spends around 26k gas per response. A successful counter leads to the forfeiture of the challenger’s bond, which is transferred to the aggregator as compensation. These results demonstrate that the protocol effectively deters unproductive disputes while preserving correctness through verifiable commitments.

5.3 Cost and Latency Analysis

We compare four protocol variants: SettleFL-CC, SettleFL-CC-Sol, SettleFL-CP, and BCFL. Figure 9 reports the average gas cost and latency per round. Specifically, the gas cost is computed over experiments with 10, 50, 100, and 200 training rounds, and the latency is evaluated under the 10 and 50 round settings. Proofs, when required, were generated using rapidsnark [32].

As shown in Figure 9(a), both SettleFL-CC and SettleFL-CC-Sol maintain stable gas cost across rounds and participants. SettleFL-CP has constant but higher cost due to per-round proofs. BCFL scales linearly and soon becomes impractical. Latency is estimated under two block times: 1s to simulate fast chains, and 12s to reflect Ethereum’s average. SettleFL-CC and SettleFL-CC-Sol stay efficient

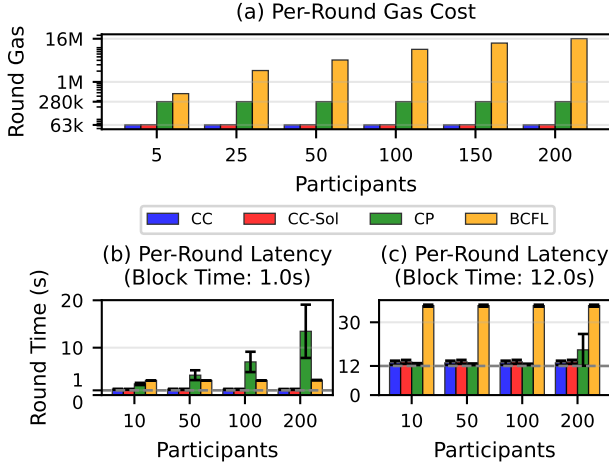


Figure 9: Per-round cost and latency comparison. SettleFL variants achieve stable gas usage and low latency.

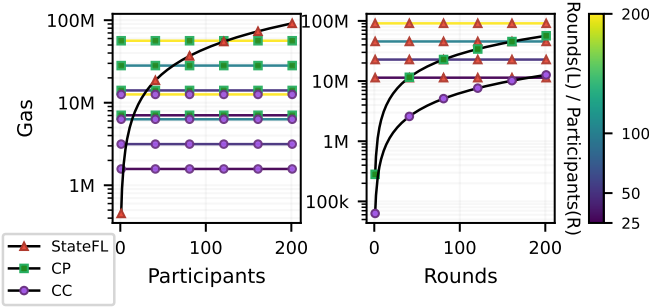


Figure 10: Gas cost comparison of StateFL and SettleFL. StateFL incurs 456k gas per participant. Conversely, SettleFL-CC and SettleFL-CP cost 63k and 281k gas per round, remaining more efficient except in high-round, low-participant settings.

in both cases. SettleFL-CP suffers from proof delays, and its latency grows with the number of rounds, leading to larger error bars. BCFL accumulates on-chain bottlenecks.

Results confirm that the SettleFL family achieves low and predictable cost and latency, outperforming other designs.

Comparison to Prior Works. OpenFL [42] extends BCFL with a feedback mechanism, but its baseline gas cost remains in the same order of magnitude as BCFL. StateFL [26] instead relies on Perun [14] state channels. Since its original paper did not report consistent gas values, we re-implemented its workflow using the same stack and measured its per-participant cost. StateFL is round-invariant but scales linearly in participants, whereas SettleFL is participant-invariant but grows with rounds. Figure 10 summarizes the trade-off.

5.4 Ablation Study

To evaluate the impact of SNARK verification, we compare two versions of our protocol: SettleFL-CC, which uses SNARKs to offload computation off-chain, and SettleFL-CC-Sol, a non-SNARK variant that performs all logic directly in the smart contract.

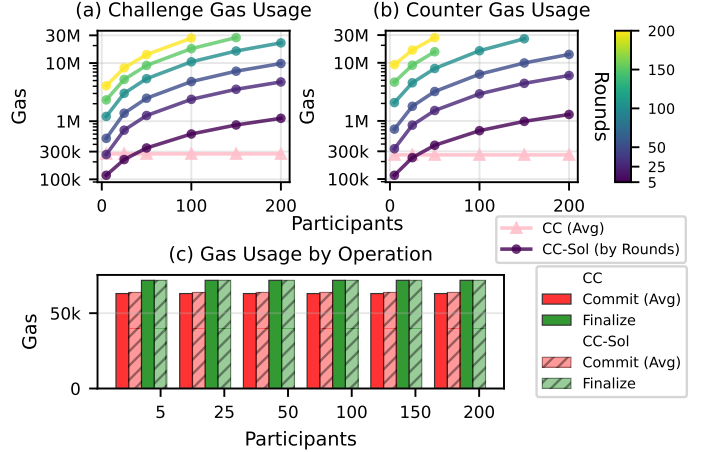


Figure 11: Gas cost of SettleFL-CC and SettleFL-CC-Sol.

While both versions implement the same commit semantics, they differ in cryptographic primitives and execution models. SettleFL-CC relies on SNARK-friendly primitives (Poseidon, EdDSA) and constant-size proofs, whereas SettleFL-CC-Sol uses Ethereum-native operations (Keccak, ECDSA) with variable cost based on input size.

Figure 11 shows the gas cost comparison across challenge and counter phases. We observe that when SNARKs are used, the gas cost remains constant regardless of the number of participants or rounds. In contrast, the non-SNARK implementation incurs a gas cost that grows linearly with the number of verifications. Due to Ethereum’s per-transaction gas limit (2^{24}), extremely large SettleFL-CC-Sol configurations exceed the threshold and are omitted from the plot.

Although SettleFL-CC incurs a higher base cost due to proof verification, it outperforms SettleFL-CC-Sol in most practical settings, especially as the number of participants or training rounds increases. The non-SNARK variant offers only marginal gas savings in small-scale deployments, such as settings with fewer than 25 participants and fewer than 5 rounds. In contrast, the gas cost of SettleFL-CC-Sol is dynamic and depends on the input size, whereas SettleFL-CC maintains a constant cost thanks to the fixed overhead of the Groth16 verifier.

These results confirm that SNARK-based offloading yields predictable and scalable cost profiles, making it a more robust choice for large-scale FL deployments. In addition, the use of SNARK preserves privacy by avoiding on-chain exposure of detailed intermediate states or participant contributions which may benefit future work.

5.5 Scalability Evaluation

Our protocol achieves constant per-round cost for training and commitment, making reward distribution the sole scalability bottleneck. In this section, we evaluate how far SettleFL can scale in terms of blockchain deployment limits and off-chain proof cost.

Scalability Boundaries. We evaluate the system at scale by simulating reward distribution for up to 800 participants. Ethereum enforces a maximum transaction gas limit of 2^{24} and restricts smart contract bytecode to 24KB. While gas limits can be mitigated via

Table 3: Constraint count and average proof generation time for main circuits across different backends and configurations.

Circuit	50 rounds					100 rounds					200 rounds				
	Cnstr.	I-GPU	I-CPU	S-CPU	R-CPU	Cnstr.	I-GPU	I-CPU	S-CPU	R-CPU	Cnstr.	I-GPU	I-CPU	S-CPU	R-CPU
challenge	1.1/1.8	0.6/1.1	26/41	46/79	6.5/11	2.2/3.5	1.2/2.2	46/77	86/147	12/21	4.3/6.9	2.4/11	84/142	165/282	24/41
transition	2.2/3.4	1.2/2.2	47/79	86/146	12/21	4.3/6.8	2.4/11	84/142	163/286	23/40	8.4/13.5	12/AF	161/281	314/585	43/83
distribute-1s	1.1/1.8	0.6/1.1	26/41	46/78	6.6/11	2.2/3.5	1.2/2.2	44/75	85/147	12/21	4.3/6.9	2.4/11	85/141	171/288	23/41
distribute-ms	1.1/1.8	0.6/1.1	26/39	46/78	6.7/12	2.2/3.5	1.2/2.1	46/75	85/148	13/22	4.3/6.9	2.4/11	86/144	164/281	24/41

Note. Runtime results (I-GPU, I-CPU, S-CPU, R-CPU) are reported in seconds, with each cell showing two values corresponding to runs with 500 and 800 \mathcal{P} , respectively. Results are averaged over 10 runs. The Cnstr. column reports the number of non-linear constraints (in millions).

Backends. I-GPU: icicle-snark (GPU), I-CPU: icicle-snark (CPU), S-CPU: snarkjs, R-CPU: rapidsnark.

Abbreviations. AF: allocation failure.

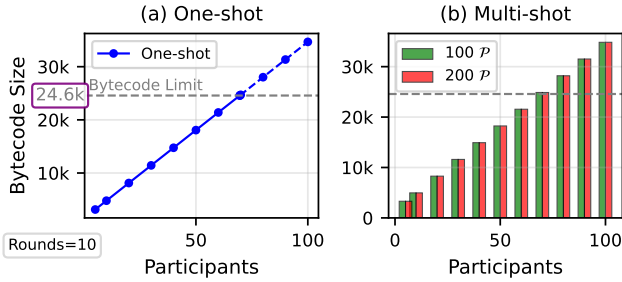


Figure 12: Bytecode size comparison between one-shot and multi-shot variants. The horizontal dashed line marks the 24KB maximum contract size allowed on Ethereum.

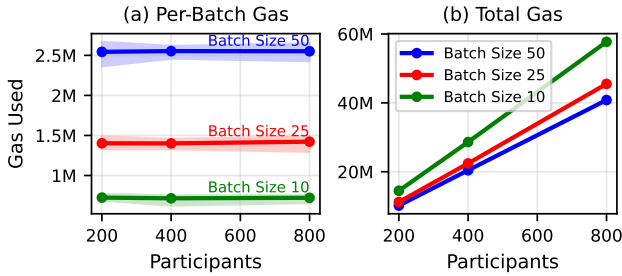


Figure 13: Multi-shot variant scalability up to 800 \mathcal{P} . Per-batch gas is invariant to total \mathcal{P} , while total gas scales linearly.

batching, we find that the bytecode size is a stricter bottleneck. Our deployment tests indicate that batch sizes exceeding 70 participants lead to contract failure regardless of available gas. Therefore, the multi-shot variant must operate with batch sizes below this threshold to remain deployable. As shown in Figure 12, the bytecode size of the multi-shot variant depends on the per-batch size rather than the total number of participants. This decoupling ensures the contract remains within the deployable bounds even under large workloads.

System Performance at Scale. Complementing the deployment analysis, Figure 13 evaluates the corresponding on-chain gas consumption. The results confirm the economic viability of the multi-shot variant at scale. For instance, with a batch size of 50, the system requires 16 on-chain transactions to complete all 800 payouts, consuming less than 41M gas in total. This configuration fits within Ethereum limits and represents a practical trade-off between contract complexity and the number of on-chain calls.

SNARK Proof Overhead. We evaluate the performance of SNARK proof generation across multiple backends, including both GPU- and CPU-based implementations. For GPU-accelerated benchmarking, we use icicle-snark [41], tested on a server equipped with eight NVIDIA RTX 4090 GPUs. Due to current implementation constraints, icicle-snark currently utilizes only a single GPU. For CPU-based benchmarks, we include rapidsnark [32] (C++), snarkjs [3] (WebAssembly), and the CPU backend of icicle-snark.

Table 3 reports the average proof generation time over 10 runs for each backend and circuit. For the configuration with 800 participants and 200 rounds, the largest circuit (used in the counter function) exceeds the available GPU memory under icicle-snark, resulting in an allocation failure (AF) error. Nonetheless, for smaller configurations (e.g., 500 participants and 200 rounds), GPU-based backends complete proof generation within seconds, confirming the practical feasibility of our design under realistic settings.

6 CONCLUSION AND FUTURE WORK

In this work, we presented SettleFL, a trustless and scalable reward settlement protocol that reconciles the high-frequency demands of FL with the scalability constraints of permissionless blockchains. Guided by the *Fundamental SettleFL Inequality*, SettleFL minimizes total economic friction through a dual-variant protocol design backed by a novel domain-specific circuit architecture. By offering interoperable optimistic and validity-based settlement paths, the protocol flexibly adapts to varying cost-latency trade-offs. Our deployment on the Ethereum Sepolia testnet confirms that SettleFL effectively breaks the scalability barrier, supporting 800 participants with negligible gas costs. Future work includes enhancing reward fairness via advanced contribution estimation, comparing with other proving systems such as STARKs or recursive proofs, and leveraging historical incentive data to enhance participant reputation credibility in dynamic FL deployments.

REFERENCES

- [1] Revin Naufal Alief, Made Adi Paramartha Putra, Augustin Gohil, Jae-Min Lee, and Dong-Seong Kim. 2023. FLB2: Layer 2 Blockchain Implementation Scheme on Federated Learning Technique. In *2023 International Conference on Artificial Intelligence in Information and Communication (ICAIC)*. 846–850. <https://doi.org/10.1109/ICAIC57133.2023.10067038>
- [2] arnaucube. 2021. Keccak256-Circom. Vocdoni. <https://github.com/vocdoni/keccak256-circom>
- [3] Jordi Baylina and iden3. 2018. Snarkjs: zkSNARK Implementation in JavaScript & WASM. <https://github.com/iden3/snarkjs>
- [4] Marta Bellés-Muñoz, Miguel Isabel, Jose Luis Muñoz-Tapia, Albert Rubio, and Jordi Baylina. 2023. Circom: A Circuit Description Language for Building Zero-Knowledge Applications. *IEEE Trans. Dependable Secur. Comput.* 20, 6 (Nov. 2023), 4733–4751. <https://doi.org/10.1109/TDSC.2022.3232813>
- [5] Eli Ben-Sasson, Alessandro Chiesa, Daniel Genkin, Eran Tromer, and Madars Virza. 2013. SNARKs for C: Verifying Program Executions Succinctly and in Zero Knowledge. In *Advances in Cryptology – CRYPTO 2013*. Springer, Berlin, Heidelberg, 90–108. https://doi.org/10.1007/978-3-642-40084-1_6
- [6] Daniel J. Bernstein, Niels Duif, Tanja Lange, Peter Schwabe, and Bo-Yin Yang. 2011. High-Speed High-Security Signatures. In *Cryptographic Hardware and Embedded Systems – CHES 2011*. Springer, Berlin, Heidelberg, 124–142. https://doi.org/10.1007/978-3-642-23951-9_9
- [7] Sebastian Caldas, Sai Meher Karthik Duddu, Peter Wu, Tian Li, Jakub Konečný, H. Brendan McMahan, Virginia Smith, and Ameet Talwalkar. 2019. LEAF: A Benchmark for Federated Settings. <https://doi.org/10.48550/arXiv.1812.01097>
- [8] Ruonan Chen, Ye Dong, Yizhong Liu, Tingyu Fan, Dawei Li, Zhenyu Guan, Jianwei Liu, and Jianying Zhou. 2025. FLock: Robust and Privacy-Preserving Federated Learning Based on Practical Blockchain State Channels. In *Proceedings of the ACM on Web Conference 2025*. Association for Computing Machinery, New York, NY, USA, 884–895. <https://doi.org/10.1145/3696410.3714666>
- [9] Yiwei Chen, Kaiyu Li, Guoliang Li, and Yong Wang. 2024. Contributions Estimation in Federated Learning: A Comprehensive Experimental Evaluation. *Proceedings of the VLDB Endowment* 17, 8 (April 2024), 2077–2090. <https://doi.org/10.14778/3659437.3659459>
- [10] Miguel Costa-Gomes, Vincent P. Crawford, and Bruno Broseta. 2001. Cognition and Behavior in Normal-Form Games: An Experimental Study. *Econometrica* 69, 5 (2001), 1193–1235. <https://doi.org/10.1111/1468-0262.00239>
- [11] Li Deng. 2012. The MNIST Database of Handwritten Digit Images for Machine Learning Research [Best of the Web]. *IEEE Signal Processing Magazine* 29, 6 (Nov. 2012), 141–142. <https://doi.org/10.1109/MSP.2012.2211477>
- [12] Harsh Bimal Desai, Mustafa Safa Ozdayi, and Murat Kantarcioglu. 2021. BlockFLA: Accountable Federated Learning via Hybrid Blockchain Architecture. In *Proceedings of the Eleventh ACM Conference on Data and Application Security and Privacy*. ACM, Virtual Event USA, 101–112. <https://doi.org/10.1145/3422337.3447837>
- [13] Meryem Malak Dif, Mouhamed Amine Bouchiha, Mourad Rabah, and Yacine Ghamri-Doudane. 2025. AutoDFL: A Scalable and Automated Reputation-Aware Decentralized Federated Learning. <https://doi.org/10.48550/arXiv.2501.04331>
- [14] Stefan Dziembowski, Lisa Ecekey, Sebastian Faust, and Daniel Malinowski. 2017. Perun: Virtual Payment Hubs over Cryptocurrencies. <https://eprint.iacr.org/2017/635>
- [15] Sizheng Fan, Hongbo Zhang, Yuchen Zeng, and Wei Cai. 2021. Hybrid Blockchain-Based Resource Trading System for Federated Learning in Edge Computing. *IEEE Internet of Things Journal* 8, 4 (Feb. 2021), 2252–2264. <https://doi.org/10.1109/JIOT.2020.3028101>
- [16] Ankit Gangwal, HariPriya Ravali Gangavalli, and Apoorva Thirupathi. 2023. A Survey of Layer-two Blockchain Protocols. *Journal of Network and Computer Applications* 209 (Jan. 2023), 103539. <https://doi.org/10.1016/j.jnca.2022.103539>
- [17] Alec Go, Richa Bhayani, and Lei Huang. 2009. *Twitter Sentiment Classification Using Distant Supervision*. Technical Report. CS224N project report, Stanford.
- [18] Ian Goodfellow, Yoshua Bengio, and Aaron Courville. 2016. *Deep Learning*. MIT Press.
- [19] Lorenzo Grassi, Dmitry Khovratovich, Christian Rechberger, Arnab Roy, and Markus Schofnegger. 2021. Poseidon: A New Hash Function for {Zero-Knowledge} Proof Systems. In *30th USENIX Security Symposium (USENIX Security 21)*. 519–535. <https://www.usenix.org/conference/usenixsecurity21/presentation/grassi>
- [20] Jens Groth. 2016. On the Size of Pairing-based Non-interactive Arguments. <https://eprint.iacr.org/2016/260>
- [21] Ehsan Hallaji, Roozbeh Razavi-Far, Mehrdad Saif, Boyu Wang, and Qiang Yang. 2024. Decentralized Federated Learning: A Survey on Security and Privacy. *IEEE Transactions on Big Data* 10, 2 (April 2024), 194–213. <https://doi.org/10.1109/TBDATA.2024.3362191>
- [22] Rong Han, Zheng Yan, Xueqin Liang, and Laurence T. Yang. 2022. How Can Incentive Mechanisms and Blockchain Benefit with Each Other? A Survey. *ACM Comput. Surv.* 55, 7 (Dec. 2022), 136:1–136:38. <https://doi.org/10.1145/3539604>
- [23] Kaiming He, Xiangyu Zhang, Shaoqing Ren, and Jian Sun. 2016. Deep Residual Learning for Image Recognition. In *2016 IEEE Conference on Computer Vision and Pattern Recognition (CVPR)*. 770–778. <https://doi.org/10.1109/CVPR.2016.90>
- [24] Md Kamrul Hossain, Walid Aljoby, Anis Elgabli, Ahmed M. Abdelmoniem, and Khaled A. Harras. 2025. AdRo-FL: Informed and Secure Client Selection for Federated Learning in the Presence of Adversarial Aggregator. <https://doi.org/10.48550/arXiv.2506.17805>
- [25] Wenke Huang, Mang Ye, Zekun Shi, Guancheng Wan, He Li, Bo Du, and Qiang Yang. 2024. Federated Learning for Generalization, Robustness, Fairness: A Survey and Benchmark. *IEEE Transactions on Pattern Analysis and Machine Intelligence* 46, 12 (Dec. 2024), 9387–9406. <https://doi.org/10.1109/TPAMI.2024.3418862>
- [26] Ioana Paula Iacoban. 2024. *StateFL: State Channels Powered Federated Learning*. Master’s thesis. Delft University of Technology.
- [27] Armand Joulin, Edouard Grave, Piotr Bojanowski, and Tomas Mikolov. 2017. Bag of Tricks for Efficient Text Classification. In *Proceedings of the 15th Conference of the European Chapter of the Association for Computational Linguistics: Volume 2, Short Papers*. Association for Computational Linguistics, Valencia, Spain, 427–431. <https://aclanthology.org/E17-2068/>
- [28] Thomas N. Kipf and Max Welling. 2017. Semi-Supervised Classification with Graph Convolutional Networks. In *International Conference on Learning Representations*. <https://openreview.net/forum?id=SJU4ayYgl>
- [29] Alex Krizhevsky. 2009. Learning Multiple Layers of Features from Tiny Images. (2009).
- [30] Y. Lecun, L. Bottou, Y. Bengio, and P. Haffner. 1998. Gradient-Based Learning Applied to Document Recognition. *Proc. IEEE* 86, 11 (Nov. 1998), 2278–2324. <https://doi.org/10.1109/5.726791>
- [31] Ji Liu, Chunlu Chen, Yu Li, Lin Sun, Yulun Song, Jingbo Zhou, Bo Jing, and Dejing Dou. 2024. Enhancing Trust and Privacy in Distributed Networks: A Comprehensive Survey on Blockchain-Based Federated Learning. *Knowledge and Information Systems* 66, 8 (Aug. 2024), 4377–4403. <https://doi.org/10.1007/s10115-024-02117-3>
- [32] Oleh Lomaka, Aleksandr Brezhnev, and Jordi Baylina. 2025. Rapidsnark. iden3. <https://github.com/iden3/rapidsnark>
- [33] Lingjuan Lyu, Xinyi Xu, Qian Wang, and Han Yu. 2020. Collaborative Fairness in Federated Learning. In *Federated Learning: Privacy and Incentive*. Springer International Publishing, Cham, 189–204. https://doi.org/10.1007/978-3-030-63076-8_14
- [34] Andrew Kachites McCallum, Kamal Nigam, Jason Rennie, and Kristie Seymore. 2000. Automating the Construction of Internet Portals with Machine Learning. *Information Retrieval* 3, 2 (July 2000), 127–163. <https://doi.org/10.1023/A:1009953814988>
- [35] Sérgio Moro, Paulo Cortez, and Paulo Rita. 2014. A Data-Driven Approach to Predict the Success of Bank Telemarketing. *Decision Support Systems* 62 (June 2014), 22–31. <https://doi.org/10.1016/j.dss.2014.03.001>
- [36] Roger B. Myerson. 1992. On the Value of Game Theory in Social Science. *Rationality and Society* 4, 1 (1992), 62–73. <https://ideas.repec.org/a/sae/ratsoc/v4y1992i1p62-73.html>
- [37] Satoshi Nakamoto. 2008. Bitcoin: A Peer-to-Peer Electronic Cash System. (2008), 9. <https://bitcoin.org/bitcoin.pdf>
- [38] Saha Reno and Koushik Roy. 2025. Navigating the Blockchain Trilemma: A Review of Recent Advances and Emerging Solutions in Decentralization, Security, and Scalability Optimization. *Computers, Materials & Continua* 84, 2 (2025), 2061–2119. <https://doi.org/10.32604/cmc.2025.066366>
- [39] Cosimo Sguanci, Roberto Spatafora, and Andrea Mario Vergani. 2021. Layer 2 Blockchain Scaling: A Survey. <https://doi.org/10.48550/arXiv.2107.10881>
- [40] Daniel Smilkov, Nikhil Thorat, Yannick Assogba, Ann Yuan, Nick Kreeger, Ping Yu, Kangyi Zhang, Shanqing Cai, Eric Nielsen, David Soergel, Stan Bileschi, Michael Terry, Charles Nicholson, Sandeep N. Gupta, Sarah Sirajuddin, D. Sculley, Rajat Monga, Greg Corrado, Fernanda B. Viégas, and Martin Wattenberg. 2019. TensorFlow.js: Machine Learning for the Web and Beyond. <https://doi.org/10.48550/arXiv.1901.05350>
- [41] Emir Soyuturk. 2025. Icicle-Snark. Ingonyama. <https://github.com/ingonyamazk/icicle-snark>
- [42] Anton Wahrstätter, Sajjad Khan, and Davor Svetinovic. 2024. OpenFL: A Scalable and Secure Decentralized Federated Learning System on the Ethereum Blockchain. *Internet of Things* 26 (July 2024), 101174. <https://doi.org/10.1016/j.iot.2024.101174>
- [43] Tianhao Wang, Johannes Rausch, Ce Zhang, Ruoxi Jia, and Dawn Song. 2020. A Principled Approach to Data Valuation for Federated Learning. In *Federated Learning: Privacy and Incentive*. Springer International Publishing, Cham, 153–167. https://doi.org/10.1007/978-3-030-63076-8_11
- [44] Jiasi Weng, Jian Weng, Jilian Zhang, Ming Li, Yue Zhang, and Weiqi Luo. 2021. DeepChain: Auditable and Privacy-Preserving Deep Learning with Blockchain-Based Incentive. *IEEE Transactions on Dependable and Secure Computing* 18, 5 (Sept. 2021), 2438–2455. <https://doi.org/10.1109/TDSC.2019.2952332>
- [45] Han Xiao, Kashif Rasul, and Roland Vollgraf. 2017. Fashion-MNIST: A Novel Image Dataset for Benchmarking Machine Learning Algorithms. <https://doi.org/10.48550/arXiv.1708.07747>

- [46] Zhibo Xing, Zijian Zhang, Ziang Zhang, Zhen Li, Meng Li, Jiamou Liu, Zongyang Zhang, Yi Zhao, Qi Sun, Liehuang Zhu, and Giovanni Russello. 2026. Zero-Knowledge Proof-based Verifiable Decentralized Machine Learning in Communication Network: A Comprehensive Survey. *IEEE Communications Surveys & Tutorials* 28 (2026), 985–1024. <https://doi.org/10.1109/COMST.2025.3561657>
- [47] Chenhao Xu, Youyang Qu, Peter W. Eklund, Yong Xiang, and Longxiang Gao. 2021. BAFL: An Efficient Blockchain-Based Asynchronous Federated Learning Framework. In *2021 IEEE Symposium on Computers and Communications (ISCC)*. 1–6. <https://doi.org/10.1109/ISCC53001.2021.9631405>

A CIRCUIT GADGETS

Algorithm 2: Gadgets

```

1 gadget  $LPI(x) \rightarrow (\vec{y})$   $\triangleright \vec{y} = (\{1\}^x, \{0\}^{T-x})$ 
2    $\forall i \in [T], y_i \leftarrow \mathbf{1}[i < x];$ 
3    $\langle \sum_{i=0}^{T-1} y_i = x \rangle;$   $\triangleright$  sum equals the integer
4    $\forall i \in [T], \langle y_i \cdot (y_i - 1) = 0 \rangle;$   $\triangleright$  booleanity
5    $\forall i \in [T + 1], \langle c_i \leftarrow \begin{cases} 1 - y_i & \text{if } i = 0 \\ y_{i-1} & \text{if } i = T \\ y_{i-1} - y_i & \text{otherwise} \end{cases} \rangle;$ 
6    $\langle \sum_{i=0}^T c_i = 1 \rangle;$   $\triangleright$  exactly one  $1 \rightarrow 0$  transition
7 gadget  $ISZERO(x) \rightarrow (y)$   $\triangleright y = \mathbf{1}[x = 0]$ 
8    $inv \leftarrow (x = 0 ? 0 : x^{-1});$ 
9    $\langle x \cdot inv = 1 - y \rangle, \langle x \cdot y = 0 \rangle;$ 
10 gadget  $H_M(\vec{x}, \rho) \rightarrow (y)$   $\triangleright$  Modular hash
11    $k \leftarrow \lfloor \frac{N}{\kappa - 1} \rfloor, y \leftarrow \rho;$ 
12   for  $i \leftarrow 0$  to  $k - 1$  do
13      $m \leftarrow \min(N - i \cdot (\kappa - 1), \kappa - 1);$ 
14      $\forall j \in [m], \langle s_j \leftarrow x_{i \cdot (\kappa - 1) + j} \rangle;$ 
15      $\langle y \leftarrow H_{m+1}(y, s_0, \dots, s_{m-1}) \rangle;$ 
16 gadget  $BATCHEXTRACTOR(\vec{x}, a) \rightarrow (\vec{y})$   $\triangleright \vec{y} = \{x_{aB}, \dots, x_{aB+B-1}\}$ 
17    $t \leftarrow \lfloor N/B \rfloor;$ 
18    $\forall i \in [t], \langle e_i \leftarrow ISZERO(a - i) \rangle;$ 
19   for  $k \leftarrow 0$  to  $t \cdot B - 1$  do
20      $i \leftarrow \lfloor k/B \rfloor, j \leftarrow k \bmod B;$ 
21      $\langle S[i][j] \leftarrow \begin{cases} x_k \cdot e_i & (k < N) \\ 0 & (\text{otherwise}) \end{cases} \rangle;$ 
22    $\forall j \in [B], \langle y_j \leftarrow \sum_{i=0}^{t-1} S[i][j] \rangle;$ 
23 gadget  $SUMROW(X, \vec{r}) \rightarrow (\vec{y})$ 
24    $\forall i \in [n], \langle y_i \leftarrow \sum_{t=0}^{T-1} X[i][t] \cdot r_t \rangle;$ 
25 gadget  $MASKCHECK(X, \vec{r})$ 
26    $\forall (i, t) \in [n] \times [T], \langle X[i][t] \cdot (1 - r_t) = 0 \rangle;$ 
27 gadget  $H_{PK}(A) \rightarrow (h_{\mathcal{A}})$ 
28    $\langle h_{\mathcal{A}} \leftarrow H_2(A_x, A_y) \rangle;$ 
29 gadget  $VERIFYCOMMITMENT(V, \mathcal{P}, \rho, A, \sigma_C) \rightarrow (C)$ 
30    $\langle C \leftarrow H_3(H_M(\text{vec}(V)), H_M(\mathcal{P}), \rho) \rangle;$ 
31    $\langle \text{EdDSA.verify}(A, \sigma_C, C) = 1 \rangle;$ 

```

B MAIN VERIFIERS

Algorithm 3: Main Verifier Circuits

```

1 circuit  $verify_{\text{transition}}(\underline{r}, V_2, \vec{p}_2, p_1, \rho, A, \sigma_{C_1}, \sigma_{C_2}) \rightarrow (\underline{C}_1, \underline{C}_2, h_{\mathcal{A}})$ 
2    $\langle \vec{r}_2 \leftarrow LPI(\underline{r} + 1) \rangle;$ 
3    $\langle \text{MASKCHECK}(\vec{r}_2, V_2) \rangle;$   $\triangleright$  Verify  $V_2$  belongs to round  $\underline{r} + 1$ 
4    $\langle \vec{r}_1 \leftarrow LPI(\underline{r}) \rangle;$   $\nabla$  Derive  $V_1$  from  $V_2$  (round  $\underline{r}$  slice)
5    $\forall (i, t) \in [n] \times [T], \langle V_1[i][t] \leftarrow V_2[i][t] \cdot \vec{r}_1[t] \rangle;$ 
6    $\langle \vec{r}_{p_1} \leftarrow LPI(p_1) \rangle;$ 
7    $\forall i \in [n], \langle \vec{p}_1[i] \leftarrow \vec{p}_2[i] \cdot \vec{r}_{p_1}[i] \rangle;$   $\triangleright$  Derive  $\vec{p}_1$  from  $\vec{p}_2$ 
8    $\langle h_{\mathcal{A}} \leftarrow H_{PK}(A) \rangle;$ 
9    $\forall i \in \{1, 2\}, \langle \underline{C}_i \leftarrow \text{VERIFYCOMMITMENT}(V_i, \vec{p}_i, \rho, A, \sigma_{C_i}) \rangle;$ 
10 circuit  $verify_{\text{challenge}}(\underline{r}, V, \vec{p}, \rho, A, \sigma_C) \rightarrow (C, h_{\mathcal{A}})$ 
11    $\langle \vec{r} \leftarrow LPI(\underline{r}) \rangle;$ 
12    $\langle \text{MASKCHECK}(\vec{r}, V) \rangle;$   $\triangleright$  Verify  $V$  belongs to round  $\underline{r} + 1$ 
13    $\langle h_{\mathcal{A}} \leftarrow H_{PK}(A) \rangle;$ 
14    $\langle C \leftarrow \text{VERIFYCOMMITMENT}(V, \vec{p}, \rho, A, \sigma_C) \rangle;$ 
15 circuit  $verify_{\text{distribute}}(\underline{r}, \underline{b}, V, \vec{p}, \rho, A, \sigma_C) \rightarrow (C, h_{\mathcal{A}}, \vec{s}_p, \vec{p}_p)$ 
16    $\langle \vec{r} \leftarrow LPI(\underline{r}) \rangle;$ 
17    $\langle \text{MASKCHECK}(\vec{r}, V) \rangle;$   $\triangleright$  Verify  $V$  belongs to round  $\underline{r} + 1$ 
18    $\langle \vec{s} \leftarrow \text{SUMROW}(V, \vec{r}) \rangle;$ 
19    $\langle \vec{p}_p \leftarrow \text{BATCHEXTRACTOR}(\vec{p}, \underline{b}) \rangle;$ 
20    $\langle \vec{s}_p \leftarrow \text{BATCHEXTRACTOR}(\vec{s}, \underline{b}) \rangle;$ 
21    $\langle h_{\mathcal{A}} \leftarrow H_{PK}(A) \rangle;$ 
22    $\langle C \leftarrow \text{VERIFYCOMMITMENT}(V, \vec{p}, \rho, A, \sigma_C) \rangle;$ 

```

C INCENTIVE COMPATIBILITY

We formalize the incentive compatibility of our protocol by modeling the interaction as a static complete-information game. Each player selects a strategy to maximize its utility, and we show that honest behavior constitutes a Nash equilibrium [36] under rational assumptions.

Game Model. We define a one-shot normal-form game [10]:

$$\mathcal{G} = (M, \{\mathcal{S}_i\}_{i \in M}, \{u_i\}_{i \in M}),$$

where $M = \{\mathcal{A}, P_1, \dots, P_N\}$ is the set of all players, consisting of the aggregator \mathcal{A} and participants P_1, \dots, P_N . Each player $i \in M$ chooses a strategy $s_i \in \mathcal{S}_i$ to maximize its utility $u_i(s_i, s_{-i})$.

Although the overall protocol may consist of multiple training rounds, we model the interaction as a one-shot static game because the first occurrence of malicious behavior (e.g., incorrect commitment or false challenge) triggers an immediate resolution phase involving dispute handling, slashing, and final reward distribution. This effectively terminates the ongoing round-based process, making the game finite and strategically equivalent to a single-shot interaction.

Furthermore, as participants interact only with the aggregator and not with each other, their incentives can be analyzed independently. The strategy of each participant depends only on the aggregator's behavior and does not influence or depend on the actions of other participants.

Aggregator strategy space $\mathcal{S}_{\mathcal{A}}$:

- $s_{\mathcal{A}}^{\text{honest}}$: Commit correct rewards and finalize distribution.
- $s_{\mathcal{A}}^{\text{tamper}}$: Publish incorrect rewards for extra gain.
- $s_{\mathcal{A}}^{\text{abort}}$: Exit early to avoid costs.

Participant strategy space \mathcal{S}_{P_i} :

- s_i^{honest} : Train, verify, and act accordingly.
- $s_i^{\text{malicious}}$: Submit false challenge to steal rewards.
- s_i^{passive} : Skip verification to avoid cost.

Utility Function. To facilitate formal analysis, we explicitly define all associated parameters for the utility functions introduced. Each player's utility is determined by reward R , penalty P , and cost C , with binary indicators I determining which terms apply.

Aggregator \mathcal{A} :

$$u_{\mathcal{A}} = \begin{cases} R_{\mathcal{A}}^{\text{model}} + R_{\mathcal{A}}^{\text{bonus}} - C_{\mathcal{A}}^{\text{commit}} & \text{if } s_{\mathcal{A}} = s_{\mathcal{A}}^{\text{honest}} \\ R_{\mathcal{A}}^{\text{model}} - C_{\mathcal{A}}^{\text{commit}} - I_{\mathcal{A}}^{\text{caught}} \cdot P_{\mathcal{A}}^{\text{slash}} & \text{if } s_{\mathcal{A}} = s_{\mathcal{A}}^{\text{tamper}} \\ -I_{\mathcal{A}}^{\text{caught}} \cdot P_{\mathcal{A}}^{\text{slash}} & \text{if } s_{\mathcal{A}} = s_{\mathcal{A}}^{\text{abort}} \end{cases},$$

Participant P_i :

$$u_{P_i} = \begin{cases} R_i^{\text{reward}} + I_i^{\text{chal}} \cdot P_i^{\text{slash}} - C_i^{\text{gas}} & \text{if } s_{P_i} = s_{P_i}^{\text{honest}} \\ R_i^{\text{reward}} + (1 - I_i^{\text{fail}}) \cdot R_i^{\text{steal}} & \text{if } s_{P_i} = s_{P_i}^{\text{malicious}} \\ -I_i^{\text{fail}} \cdot P_i^{\text{slash}} - C_i^{\text{gas}} & \\ R_i^{\text{reward}} & \text{if } s_{P_i} = s_{P_i}^{\text{passive}} \end{cases},$$

where:

- $R_{\mathcal{A}}^{\text{bonus}}$: reward for finalizing reward distribution.
- $R_{\mathcal{A}}^{\text{model}}$: reward for \mathcal{A} achieving the desired final model.
- R_i^{reward} : reward received by P_i as incentive.
- R_i^{steal} : reward gained by P_i through successful theft.
- $P_{\mathcal{A}}^{\text{slash}}, P_i^{\text{slash}}$: penalty for caught misbehavior.
- $C_{\mathcal{A}}^{\text{commit}}, C_i^{\text{gas}}$: cost for on-chain operations.
- $I_{\mathcal{A}}^{\text{caught}}$: indicator for whether \mathcal{A} tampering is challenged by at least one participant.
- I_i^{chal} : indicator for whether P_i challenges upon detecting misbehavior.
- I_i^{fail} : indicator for whether P_i 's challenge fails.

PROOF OF THEOREM 1. Here we provide the formal proof for Theorem 1 presented in Section 4.6. We prove that the strategy profile

$$\mathbf{s}^* = (s_{\mathcal{A}}^{\text{honest}}, s_1^{\text{honest}}, \dots, s_N^{\text{honest}})$$

constitutes a Nash equilibrium of the game $\mathcal{G} = (M, \{\mathcal{S}_i\}_{i \in M}, \{u_i\}_{i \in M})$ under rational behavior.

Binary Indicator Instantiations. In the strategy profile \mathbf{s}^* , we have:

- $I_{\mathcal{A}}^{\text{caught}} = 1$, since all P_i are honest (i.e., not passive).
- $I_i^{\text{chal}} = 1$, as P_i verifies and challenges when appropriate.
- $I_i^{\text{fail}} = 1$, since \mathcal{A} is honest and counters all false challenges.

Aggregator Deviation Analysis. Assume all \mathcal{P} follow s_i^{honest} . Then:

- Honest behavior yields:

$$u_{\mathcal{A}}^{\text{honest}} = R_{\mathcal{A}}^{\text{model}} + R_{\mathcal{A}}^{\text{bonus}} - C_{\mathcal{A}}^{\text{commit}}.$$

- Tampering yields:

$$u_{\mathcal{A}}^{\text{tamper}} = R_{\mathcal{A}}^{\text{model}} - C_{\mathcal{A}}^{\text{commit}} - P_{\mathcal{A}}^{\text{slash}}.$$

- Aborting yields:

$$u_{\mathcal{A}}^{\text{abort}} = -P_{\mathcal{A}}^{\text{slash}}.$$

Since all parameters are positive, we have:

$$u_{\mathcal{A}}^{\text{honest}} > u_{\mathcal{A}}^{\text{tamper}} \quad \text{and} \quad u_{\mathcal{A}}^{\text{honest}} > u_{\mathcal{A}}^{\text{abort}}.$$

Thus, \mathcal{A} has no incentive to deviate.

Participant Deviation Analysis. Fix $s_{\mathcal{A}} = s_{\mathcal{A}}^{\text{honest}}$ and $s_j = s_j^{\text{honest}}$ for all $j \neq i$. Consider P_i :

- Honest behavior yields:

$$u_i^{\text{honest}} = R_i^{\text{reward}} + P_{\mathcal{A}}^{\text{slash}} - C_i^{\text{gas}}.$$

- Malicious behavior yields:

$$u_i^{\text{malicious}} = R_i^{\text{reward}} - P_i^{\text{slash}} - C_i^{\text{gas}}.$$

Since all parameters are positive, we have:

$$u_i^{\text{honest}} > u_i^{\text{malicious}}.$$

- Passive behavior yields:

$$u_i^{\text{passive}} = R_i^{\text{reward}}.$$

Honest behavior is strictly better if:

$$u_i^{\text{honest}} > u_i^{\text{passive}} \implies P_{\mathcal{A}}^{\text{slash}} > C_i^{\text{gas}}.$$

Conclusion. No player has an incentive to deviate from \mathbf{s}^* if the following condition holds:

$$P_{\mathcal{A}}^{\text{slash}} > C_i^{\text{gas}} \quad \text{for all } i \in M.$$

Therefore, \mathbf{s}^* is a Nash equilibrium of \mathcal{G} . \square

Example. We illustrate the above analysis with a concrete parameter setting:

- Aggregator: $R_{\mathcal{A}}^{\text{model}} = 10, R_{\mathcal{A}}^{\text{bonus}} = 4, C_{\mathcal{A}}^{\text{commit}} = 1, P_{\mathcal{A}}^{\text{slash}} = 3$.
- Participant P_i : $R_i^{\text{reward}} = 2, R_i^{\text{steal}} = 2, C_i^{\text{gas}} = 1, P_i^{\text{slash}} = 2$.

Under the strategy profile \mathbf{s}^* where all players behave honestly, we compute:

- Aggregator utility:

$$u_{\mathcal{A}}^{\text{honest}} = 10 + 4 - 1 = 13,$$

$$u_{\mathcal{A}}^{\text{tamper}} = 10 - 1 - 3 = 6,$$

$$u_{\mathcal{A}}^{\text{abort}} = -3.$$

The aggregator strictly prefers honest behavior.

- Participant utility:

$$u_i^{\text{honest}} = 2 + 3 - 1 = 4,$$

$$u_i^{\text{malicious}} = 2 - 2 - 1 = -1,$$

$$u_i^{\text{passive}} = 2.$$

Honest behavior yields the highest utility for each P_i .

- The equilibrium condition $P_{\mathcal{A}}^{\text{slash}} > C_i^{\text{gas}}$ is satisfied, as $3 > 1$.

Hence, no player has an incentive to deviate, and the strategy profile \mathbf{s}^* constitutes a Nash equilibrium.